

Bouncing transient currents and SQUID-like voltage in nanodevices at half fillingMichele Cini,^{1,2} Enrico Perfetto,³ Chiara Ciccarelli,¹ Gianluca Stefanucci,^{1,2,4} and Stefano Bellucci²¹*Dipartimento di Fisica, Università di Roma Tor Vergata, Via della Ricerca Scientifica 1, 00133 Rome, Italy*²*Laboratori Nazionali di Frascati, Istituto Nazionale di Fisica Nucleare, Via E. Fermi 40, 00044 Frascati, Italy*³*Unità CNISM, Università di Roma Tor Vergata, Via della Ricerca Scientifica 1, 00133 Rome, Italy*⁴*European Theoretical Spectroscopy Facility (ETSF)*

(Received 8 June 2009; revised manuscript received 3 August 2009; published 28 September 2009)

Nanorings asymmetrically connected to wires show different kinds of quantum interference phenomena under sudden excitations and in steady current conditions. Here, we contrast the transient current caused by an abrupt bias to the magnetic effects at constant current. A repulsive impurity can cause charge buildup in one of the arms and reverse current spikes. Moreover, it can cause transitions from laminar current flow to vortices, and also change the chirality of the vortex. The magnetic behavior of these devices is also very peculiar. Those nanocircuits, that consist of an odd number of atoms, behave in a fundamentally different manner compared to those that consist of an even number of atoms. The circuits having an odd number of sites connected to long-enough symmetric wires are diamagnetic; they display half-fluxon periodicity induced by many-body symmetry even in the absence of electron-phonon and electron-electron interactions. In principle, one can operate a kind of quantum interference device without superconductors. Since there is no gap and no critical temperature, one predicts qualitatively the same behavior at and above room temperature, although with a reduced current. The circuits with even site numbers, on the other hand, are paramagnetic.

DOI: [10.1103/PhysRevB.80.125427](https://doi.org/10.1103/PhysRevB.80.125427)

PACS number(s): 72.10.Bg, 85.25.Dg, 74.50.+r

I. INTRODUCTION

The last decade has witnessed a growing interest in the persistent currents in quantum rings threaded by a magnetic flux ϕ . This problem has many variants. The rings of interest may contain impurities or may interact with quantum dots or reservoirs. Moreover, both continuous and discrete formulations have been used, to date, with similar results. Aligia¹ modeled the persistent currents in a ring with an embedded quantum dot. Theoretical approaches to one-dimensional and quasi-one-dimensional quantum rings with a few electrons are reviewed by Viefers *et al.*² See also the recent review by Maiti,³ where it is pointed out that central issues such as the diamagnetic or the paramagnetic sign of the low-field currents of isolated rings are still unsettled. The present paper, instead, is devoted to rings connected to circuits. It is clear that the connection to wires substantially modifies the problem, but here we point out that some of the modifications are not obvious and lead to quite interesting consequences.

Simple quantum rings can be connected to biased wires in such a way that the current flows through inequivalent paths. In the present exploratory paper, we consider a tight-binding ring with N sites attached to two one-dimensional leads and specialize on the half-filled system. We show that this innocent-looking situation produces peculiar phenomena like *bouncing transients*, i.e., current spikes in the reverse direction, and a sort of simulated pairing. These systems could find applications in spintronic or fast electronic devices exploiting spikes in the onset currents, or also in steady current conditions, when used to measure local magnetic fields. Thus, our motivation is twofold. On one hand, we look for the conditions that can produce novel phenomena in the transient current when the system is biased. On the other hand, we are interested in the bias that develops across the system in steady current conditions when it is used like a supercon-

ducting quantum interference device (SQUID). After presenting the model in Sec. II, in Sec. III we present the formalism, and in Sec. IV apply it to situations where transient currents through the circuit are large and appear to bounce to a direction contrary to the main stream. We then discuss the currents inside the device, with vortices that can be clockwise or counterclockwise depending on the parameters. The nontrivial topology allows interference effects of the Aharonov-Bohm type in one-body experiments, but in addition, a many-body symmetry comes into play when the ring has an odd number of atoms. The interplay of symmetry and topology may lead to a diamagnetic behavior with a half-fluxon periodicity that looks like a typical superconducting pattern as shown in Sec. V. The possible operation of the circuit as a magnetometer is also suggested. Our main results are summarized in the concluding Sec. VI.

II. MODEL

The Hamiltonian describing the left (L) and right (R) one-dimensional leads is

$$H_\alpha = t_h \sum_{m=0}^{\infty} (c_{m,\alpha}^\dagger c_{m+1,\alpha} + \text{H.c.}), \quad (1)$$

where t_h is the hopping integral between nearest-neighbor sites and $c_{m+1,\alpha}$ annihilates an electron at site $m+1$ in wire $\alpha=L, R$. The spin indices are not shown in order to simplify the notation. The energy window of both L and R continua is $(-2|t_h|, 2|t_h|)$, and the half-filled system corresponds to having a chemical potential $\mu=0$. In this work, we consider N -sided polygonal devices described by the Hamiltonian

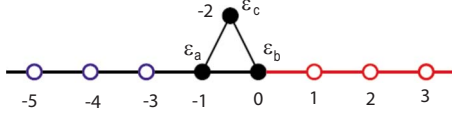


FIG. 1. (Color online) Sketch of the site numbering and site energies of the triangular ring, shown with part of the leads. The impurity is denoted by its energy ϵ_c , while we shall set $\epsilon_a = \epsilon_b = 0$. The hopping integrals in the absence of magnetic field are $t_{ab} = t_{bc} = t_{ca} = t_{dev}$.

$$H_{\text{ring}} = \sum_{\langle m,n \rangle=1}^N t_{mn} d_m^\dagger d_n, \quad (2)$$

where d_n are Fermion annihilation operators inside the device and t_{mn} is the hopping between site m and site n . In the rest of the paper, we specialize to the case $t_{mn} = 0$ if m and n are not nearest neighbors and $t_{mn} \equiv t_{dev} e^{i\alpha(m,n)}$, where $e^{i\alpha(m,n)}$ is a phase factor, otherwise. The simplest example is the triangular model ($N=3$) shown in Fig. 1. In this case, we also label the sites with letters and consider a nonmagnetic impurity at the vertex site c of strength ϵ_c

$$H_{\text{ring}} = \sum_{\langle m,n \rangle \in \{a,b,c\}} t_{mn} d_m^\dagger d_n + \epsilon_c n_c, \quad (3)$$

with $n_c = d_c^\dagger d_c$.

The wires will be attached at a couple of sites in the ring that will be specified case by case below by using a tunneling Hamiltonian H_T with hopping parameter t_h . Thus, the equilibrium Hamiltonian reads

$$H_0 = H_L + H_R + H_{\text{ring}} + H_T, \quad (4)$$

while for times $t > 0$

$$H(t) = H_0 + H_{\text{bias}}(t), \quad (5)$$

where

$$H_{\text{bias}}(t) = \sum_{\alpha=L,R} \sum_{m=0}^{\infty} V_\alpha(t) n_{m,\alpha}, \quad (6)$$

with $n_{m\alpha} = c_{m\alpha}^\dagger c_{m\alpha}$. The bias shifts the energy of the α sites by a constant amount, with a time dependence $V_\alpha(t)$.

The electron number current operator between sites m and n connected by a bond with hopping integral τ_{mn} [$\tau_{mn} = t_h$ or $t_{dev} e^{i\alpha(m,n)}$ inside the device] is determined⁴ by imposing the continuity equation

$$J_{mn} = -\frac{i}{\hbar} \tau_{mn} c_n^\dagger c_m + \text{H.c.} \quad (7)$$

For ring sites, c operators will be replaced by d ones.

III. FORMALISM

In the partition-free approach⁵ the formula for the time-dependent averaged current through the m - n bond reads

$$\langle J_{mn}(t) \rangle = \text{Tr}[\hat{f}^{(0)} U^\dagger(t) J_{mn} U(t)], \quad (8)$$

with

$$\hat{f}^{(0)} = \frac{1}{e^{\beta(H_0 - \mu)} + 1}, \quad (9)$$

the Fermi function computed at the equilibrium Hamiltonian H_0 and $U(t)$ the evolution operator. In the actual calculations we have adopted a local view and write the electron number current

$$\langle J_{mn}(t) \rangle = \frac{2e}{\hbar} \text{Im} \left[\tau_{mn} \sum_{rs} \langle n | U^\dagger(t) | r \rangle \langle s | U(t) | m \rangle f(r,s) \right], \quad (10)$$

where $f(r,s) = \langle r | \hat{f}^{(0)} | s \rangle$ is the matrix element of $\hat{f}^{(0)}$ between one-particles states localized at sites r and s . In this way, we observed that far sites in the wires come into play one after another with a clear-cut delay. One can simulate infinite leads with wires consisting of l sites and obtain quite accurate currents for times up to $t = (l/3)\hbar/t_h$; the absence of more distant sites does not change the results in any appreciable measure. Eventually, when t is increased at fixed length l , the information that the wires are finite arrives quite suddenly and a fast drop of the current takes place.⁶

Another useful expression for the bond current that holds for step-function switching of the bias can be obtained by inserting into Eq. (10) complete sets ψ_1, ψ_2 , of H eigenstates (in the presence of the bias) with energy eigenvalues $E(\psi_1), E(\psi_2)$; one gets

$$\langle J_{mn}(t) \rangle = -\frac{2e}{\hbar} \text{Im} \left[t_{mn} \sum_{\psi_1, \psi_2} e^{i(E(\psi_1) - E(\psi_2))t/\hbar} \langle n | \psi_1 \rangle \times \langle \psi_2 | m \rangle \sum_{n_1, n_2} \langle \psi_1 | n_1 \rangle \langle n_2 | \psi_2 \rangle f(n_1, n_2) \right]. \quad (11)$$

This informs us about the frequency spectrum of the current response. The frequencies arise from energy differences between the eigenstates of the Hamiltonian of the full circuit with the bias included. The weights at a given bond depend in a simple way on the eigenfunctions at the bond and on the equilibrium occupation of single-electron states. If there are sharp discrete states outside the continuum, $\langle J_{mn}(t) \rangle$ has an oscillatory component,⁷ otherwise it tends⁵ to the current-voltage characteristics asymptotically as $t \rightarrow \infty$.

IV. SWITCH-ON CURRENTS

We study the triangular model of Fig. 1 with $t_{ab} = t_{bc} = t_{ca} = t_{dev}$ and $t_{dev} = t_h$ for the sake of definiteness. Our main idea in the model calculations has been to study the ϵ_c dependence of the transient in order to look for marked out-of-equilibrium behavior, like vortex formation, or large charge buildup followed by strong current spikes. Also, one is interested in conditions that produce a fast change of the response with ϵ_c , since possibly in such situations, magnetic impurities can produce strong spin polarization.

Below, we present numerical results for 150 sites in the leads (which guarantee an accurate propagation up to times $20\hbar/t_h$) and switch on a constant bias $V_L = V = 0.5$ and $V_R = 0$ at $t=0$. In the steady state, it tends to produce a negative local current flow (in the sense that the electron number current goes from the right to the left wire).

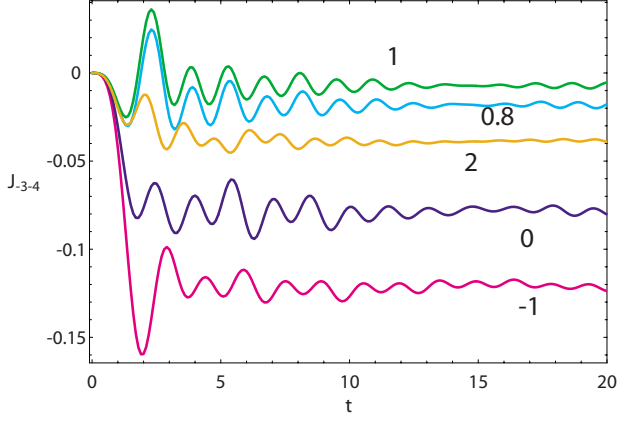


FIG. 2. (Color online) Time dependence of the current on the bond between the sites -3 and -4 . The numbers shown close to each curve indicate the values of ϵ_c . From bottom $\epsilon_c = -1, 0, 2, 0.8, 1$ in units of t_h . Here and below t is in \hbar/t_h units and the current is in units of t_h/\hbar .

A. Total current

In Fig. 2 we show the time dependence of the number current in $\frac{t_h}{\hbar}$ units on the bond between sites -3 and -4 for different values of ϵ_c .

1. Long-time limit

The times we are considering are short enough to enable us to use the finite-lead scheme specified above, however, the system already clearly approaches the steady state for all ϵ_c . The effect of the impurity at site c on the asymptotic current is much stronger than one could have expected from any classical analog. The current at $\epsilon_c = -1$ (in units of t_h) is more than an order of magnitude larger than it is at $\epsilon_c = +1$. Moreover, in a range around $\epsilon_c = 0$, the negative current increases (that is, its absolute value decreases) with increasing ϵ_c , as one could expect if the repulsive site were an obstruction to the current flow. However, this view is not in line with the fact that a further increase of ϵ_c increases the conductivity of the device. The correct interpretation is that the conductivity is ruled by quantum interference between the $a-b$ and $a-c-b$ paths, particularly by electrons around the Fermi level.

2. Short and intermediate times

Here, we are in position to see how this quantum interference develops in time. It takes a time $\sim \hbar/t_h$ for the current to go from zero to the final order of magnitude; then for some \hbar/t_h , large oscillations occur, which appear to be damped with a characteristic time $\sim 10\hbar/t_h$. The oscillations have characteristic frequencies that, in accordance with Eq. (11), increase by increasing the hopping matrix elements or modifying the device in any way that enhances the energy level differences. It can be seen that the damping of the oscillations is not exponential, and characteristic times of the order of $10t_h/\hbar$ are also noticeable.

Figure 2 shows that at $\epsilon_c = 0$, the current quickly approaches $-0.08t_h/\hbar$; but at short times, the spread of values of the currents is larger than it is at asymptotic times. A

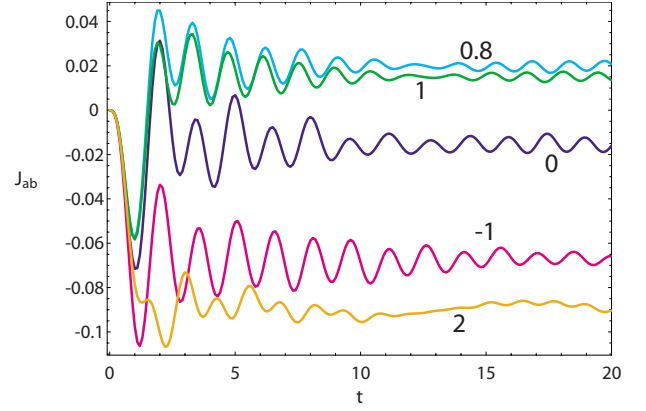


FIG. 3. (Color online) Time dependence of $\langle J_{ab} \rangle$. The numbers shown close to each curve indicate the values of ϵ_c . From bottom, $\epsilon_c = 2, -1, 0, 1, 0.8$ in units of t_h .

negative impurity like $\epsilon_c = -1$ produces a spike whose magnitude exceeds by $\sim 30\%$ the steady state value $\sim -0.12t_h/\hbar$, while a positive ϵ_c reduces the conductivity of the device. The dependence of the current on ϵ_c and time is involved, with the $\epsilon_c = 1$ case which does not belong to the region delimited by $\epsilon_c = 0$ and $\epsilon_c = 2$ curves. The $\epsilon_c = 0.8$ and $\epsilon_c = 1.0$ curves that produce small negative currents at long times are most interesting. They even go positive for some time interval $\sim \hbar/t_h$. Positive currents go backward. This bouncing current is a quantum interference effect, which takes the system temporarily but dramatically out of equilibrium and in countertrend to the steady state. The main spike of reversed current is much larger than the long-time direct current response. Next, to understand what produces the bouncing current, we look at the transport inside the triangular device.

B. Laminar flow and Vortices

In Figs. 3 and 4, we report the time-dependent $\langle J_{ab} \rangle$ and $\langle J_{bc} \rangle$ at times $0 < t < 20\hbar/t_h$ for $\epsilon_a = \epsilon_b = 0$ and various values of ϵ_c . When the site c is attractive for electrons (that is, ϵ_c

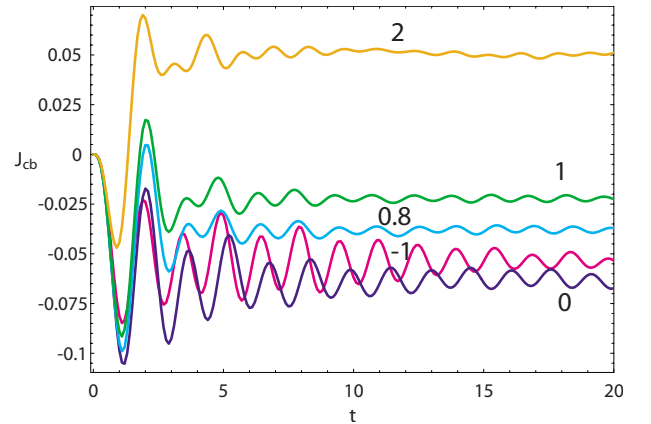


FIG. 4. (Color online) Time dependence of $\langle J_{cb} \rangle$. The numbers shown close to each curve indicate the values of ϵ_c . From bottom, $\epsilon_c = 0, -1, 0.8, 1, 2$ in units of t_h .

<0), despite some transient oscillations, the current remains negative, both on the a - b and c - b bonds; the current flows from b toward a and c , so the flow is *laminar*. The magnitude of the current on the a - b and c - b bonds is comparable. Although site c may have a high electron population, the local current does not concentrate on either bond.

For $\epsilon_c=0.8$ and $\epsilon_c=1.0$ the current J_{ab} on the a - b bond (Fig. 3), after a negative transient spike, produces a positive one, which is the main contribution to the bouncing current noted above. This behavior can be understood in terms of a strong charge buildup on the a - c - b arm of the ring during the first burst following the switching of the bias, which eventually triggers the temporary backflow. After the burst, J_{ab} remains positive ($\epsilon_c=0.8$ and $\epsilon_c=1.0$ curves in Fig. 3) while J_{cb} remains negative value ($\epsilon_c=0.8$ and $\epsilon_c=1.0$ curves in Fig. 4). In other terms, we observe the formation of an anticlockwise current *vortex*.^{8,9}

Remarkably and unexpectedly, by increasing ϵ_c one reaches a critical value beyond which the vortex becomes clockwise, as one can see from the $\epsilon_c=2$ curves in Figs. 3 and 4. This conclusion is unavoidable since the current changes sign in both arms of the circuit. The total current (Fig. 2) remains negative, as one expects. We were unable to find any simple qualitative explanation for the inversion of the vortex. In general the critical value of ϵ_c depends on the bias V and for $V=0.5$ is about 1. Moreover, we emphasize that the current across a strongly repulsive site with $\epsilon_c=2$ is still comparable in magnitude with the one on the a - b bond.

V. MANY-BODY SYMMETRY AND MAGNETIC RESPONSE

Nanoring devices asymmetrically connected to wires of Λ sites each are even more peculiar for their magnetic properties. Here, we restrict to the case $\epsilon_c=0$. The magnetic flux ϕ through the ring is inserted by the Peierls prescription^{10,11}

$$t_{ac} \rightarrow t_{ac} e^{2\pi i \alpha}, \quad (12)$$

where $\alpha = \phi/\phi_0$ and $\phi_0 = hc/e$ is the magnetic flux quantum. In the case of vanishing bias, in stationary conditions one finds a diamagnetic current which is confined to the triangular ring. In Fig. 5 we illustrate our results. We sketch a triangular device connected to 14-site leads and the ground-state energy $E_0(\alpha)$ versus $\alpha = \phi/\phi_0$ for $t_{dev} \equiv t_{ab} = t_{bc} = t_{ca} = 1, 3$, and 5. The expected periodicity in α with period 1 due to gauge invariance is of course observed. Strikingly, however, we notice that the period is actually 1/2, and the system is diamagnetic, i.e., the energy increases when the unmagnetized system is put in a magnetic field. In other terms, $E_0(\alpha)$ looks like the ground-state energy of a superconducting ring, although this is a noninteracting model and the spectrum is gapless.

One could wonder how the positive diamagnetic response at small fields arises, since the initial dependence of the total energy on the flux is quadratic and the second-order correction is always negative. However, this is an apparent paradox. The energy change is due to a perturbation $t_{dev}(e^{2\pi i \alpha} - 1) \sim t_{dev}(2\pi i \alpha - 2\pi^2 \alpha^2)$, which is the effect of changing the phase of one bond. First-order perturbation theory corre-

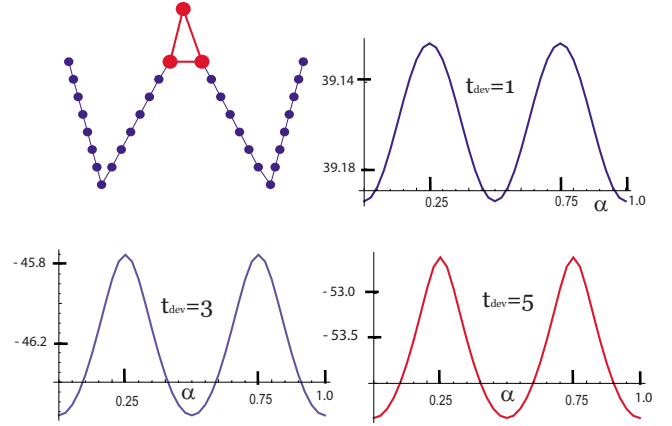


FIG. 5. (Color online) The $\phi/2$ periodicity arising from the symmetry-induced false pairing. Top left: the triangular device connected to $\Lambda=14$ -site wires. The other panels show the ground-state energy $E_0(\alpha)$ versus α . Top right: $t_{dev}=t_h$. Bottom left: $t_{dev}=3t_h$. Bottom right: $t_{dev}=5t_h$.

sponds to compute the current operator over the ground state and it is zero. The quadratic contribution is given by second-order perturbation theory in $2\pi i \alpha t_{dev}$, plus a term coming from the first-order correction in $-2\pi^2 \alpha^2 t_{dev}$. The former term is always negative while the second term can be either positive or negative.

A. Nontrivial role of the wires

The results in Fig. 5 are striking because the isolated nanoring with three sites at half-filling does not simulate any superconducting behavior; instead, it yields a paramagnetic pattern, symmetric around $\alpha = \frac{1}{2}$ ($\alpha=1$ is equivalent to $\alpha=0$). One can easily work out the lowest energy eigenvalue E_0 with three electrons. $E_0=-3$ for $\alpha=0$ sinks to $E_0=-2\sqrt{3} \sim -3.46$ at $\alpha=\frac{1}{4}$, and rises again to $E_0=-3$ at $\alpha=1/2$. Thus, there is a half-fluxon periodicity at half-filling, but $\alpha=0$ and $\alpha=1/2$ are maxima and correspond to degenerate three-body states.

The superconductorlike response requires the presence of wires, despite the fact that the diamagnetic currents induced by the field are strictly confined to the triangular device. The currents do not visit the wires, but the electron wave functions do. In order to produce the double minimum, the wires must be rather long. The barrier height $B=E_0(\frac{1}{4})-E_0(0)$ depends on the total number of atoms $\mathcal{N}=3+2\Lambda$ (see Fig. 6) and below a minimum length $B<0$. In Fig. 6, we plot the dependence of the barrier B on the number of sites $\mathcal{N}=3+2\Lambda$ of the leads. We observe that B saturates with increasing \mathcal{N} . This finding is noteworthy and unusual. The inset of Fig. 6 shows how B depends on $|t_{dev}|$ and suggests that except for an initial quadratic region, the dependence is basically linear. With hopping integrals in the eV range B easily exceeds room temperature.

B. Bipartite and not bipartite wired devices

Next, we investigate why the effect takes place in this geometry and at half-filling. A crucial observation is that the

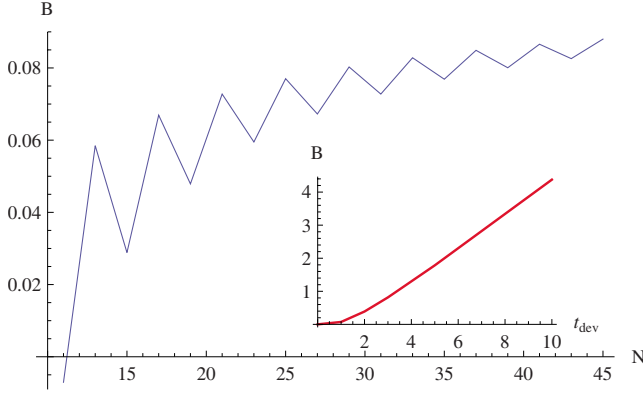


FIG. 6. (Color online) Dependence of the barrier height B on the total number N of sites, which include the triangular device and the L and R leads. The parameters are the same as in Fig. 6. The line is a guide for the eye. Note that for short leads, B is negative. The inset shows the almost linear dependence of B on $t_{dev}=t_{ab}=t_{ac}=t_{bc}$.

system depicted in Fig. 5 is not a bipartite graph. By contrast, Fig. 7 shows the flux dependence of the ground state of a bipartite graph, namely, a square device connected to wires. The response is paramagnetic since the ground state at $\phi=0$ is degenerate, the field lifts the degeneracy, a Zeeman effect occurs, and the ground-state energy is lowered. In addition, the trivial periodicity is observed.

In Fig. 8, we add one site to the device, and the diamagnetic double minimum pattern is found for the resulting pentagonal device, which does not produce a bipartite graph. Based on this observation and on a symmetry analysis, we can show that the half-fluxon periodicity ($E_0(\frac{1}{2})=E_0(0)$) holds. This is a theorem that holds for any ring with an odd number of atoms connected to leads of any length provided that the site energies vanish.

C. Symmetry analysis

Let C denote the charge-conjugation operation (or electron-hole canonical transformation) $c_\alpha \rightarrow b_\alpha^\dagger$, where c_α annihilates electrons and b_α^\dagger creates a hole with quantum numbers α . C is equivalent to $\tau_{mn} \rightarrow -\tau_{mn}$ throughout, or, since the site energies vanish, to $H \rightarrow -H$.

We recall two elementary results of graph theory: (1) an isolated ring is a bipartite graph if and only if it has an even number of atoms, and (2) adding wires of any length does not change the result.

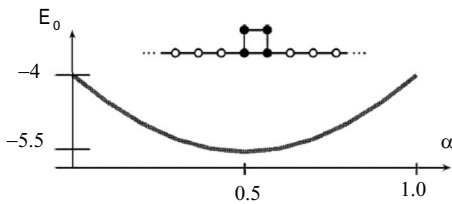


FIG. 7. Flux-dependent energy $E_0(\alpha)$ for a square device with $t_{dev}=t_h$. Notice the scale, the *paramagnetic* behavior, and the level crossing at no flux. The central part of the system, with the device and the beginning of the wires, is also shown.

In bipartite lattices, C is equivalent to a sign change of alternating orbitals, which is a gauge transformation. Hence, H and $-H$ have the same one-body spectrum, that is, the spectrum is top-down symmetric.

For the wired triangular ring and any other nonbipartite graph, the one-body spectrum is *not* top-down symmetric (except¹² at $\alpha=1/4$, $\alpha=3/4$), so it does not appear the same after the transformation, and $C:H \rightarrow -H$ is equivalent to changing the sign of one bond in the ring. But this is just the effect of the operation $F:\alpha \rightarrow \alpha+1/2$, which inserts one half of a fluxon in the ring. Therefore, the combined operation $C \circ F$ is an exact symmetry of the many-electron state which holds at half-filling. It is clear that $F:H \rightarrow -H$, i.e., F turns the spectrum upside down.

However, as noted above, the spectrum is *not* top-down symmetric and when at $\phi=\phi_0/2$ the occupied and empty spin orbitals have exchanged places, the system does not quite look like it was at $\alpha=0$. For instance, at the top of the spectrum of the device of Fig. 5 at $\alpha=0$ there is an empty split-off state. At $\alpha=0.5$ this becomes a deep state below the band. Nevertheless, we wish to prove that the many-body ground-state energy $E_0(\alpha)$ at $\alpha=1/2$ is exactly the same as at $\alpha=0$.

The reason lies in another symmetry of the many-body state at half-filling. In terms of one-body spin-orbital levels, $\text{Tr } H(\alpha)=0$ implies

$$E_0(\alpha) = \sum_i n_i(\alpha) \epsilon_i(\alpha) = - \sum_i [1 - n_i(\alpha)] \epsilon_i(\alpha). \quad (13)$$

Since under F the negative of the energy of the unoccupied levels coincide with the energy of the occupied ones, we have $\epsilon_i(\frac{1}{2}) = -\epsilon_i(0)$ and $(1 - n_i(\frac{1}{2})) = n_i(0)$ from which it follows that:

$$E_0\left(\frac{1}{2}\right) = - \sum_i (1 - n_i) \epsilon_i\left(\frac{1}{2}\right) = E_0(0). \quad (14)$$

D. Superconductor-free Quantum Interference Device

The superconducting quantum interference device consists of two superconductors separated by thin insulating layers to form two parallel Josephson junctions, and can be used as a magnetometer to detect tiny magnetic fields. If a constant biasing current is maintained in the SQUID device, the measured voltage oscillates with the change in the magnetic

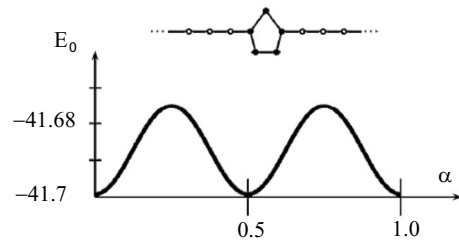


FIG. 8. Flux-dependent energy $E_0(\alpha)$ for a pentagonal device with $t_{dev}=t_h$. Notice the *diamagnetic* behavior, and the absence of level crossing at no flux. The central part of the system, with the device and the beginning of the wires, is also shown.

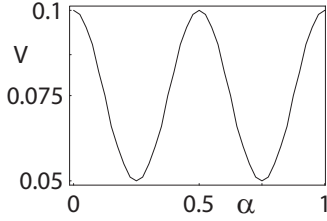


FIG. 9. Operation of the triangular device with $\epsilon_a = \epsilon_b = \epsilon_c = 0$ and $t_{dev} = t_h$ used a SQUID thread by a flux ϕ . A fixed current $J = 0.016t_h/\hbar$ flows through the device. The right wire site energies are raised by $V_R = V(\phi)$, the left wire site energies are lowered by $V_L = -V(\phi)$, and V is adjusted in order to keep J fixed. The $V(\phi)$ versus ϕ plot is perfectly periodic with a half-fluxon period and simulates a superconducting SQUID, although no superconductors are needed.

flux, and by counting the oscillations one can evaluate the flux change which has occurred. In principle one can produce Josephson-like oscillations without the need of superconductivity; if the device can be realized this can be a physical principle of interest for applications, maybe even at room temperature. Impurities and any disturbance affecting the quantum coherence can lower the operating temperature, but since in principle B can be as large as 1 eV we believe there is enough motivation for an experimental activity on this idea. According to the above arguments, the triangular pentagonal and other odd-numbered polygonal devices should simulate a SQUID, while bipartite graphs should present a normal behavior. We have performed the thought experiment with the triangular device connected to infinite wires; the results are reported in Fig. 9. We keep a fixed current J flowing through the device by adjusting $V(\phi)$, while the flux ϕ threading the device is varied. It can be seen that the plot of $V(\phi)$ versus ϕ is periodic with a half-fluxon period. The system simulates a SQUID, although no superconductors are needed. A counterexample is given in Fig. 10, where the triangular device is replaced by a square one and the effect disappears.

VI. CONCLUSIONS

We have shown that simple closed circuits have rather subtle properties when unsymmetrically connected to the biased circuit that could also be useful for designing new kinds of devices. We have found that an impurity site of energy ϵ_c in the longer arm of a triangular device can cause a transient bouncing current, which goes in the opposite direction than the long-time current and is much more intense but lasts for

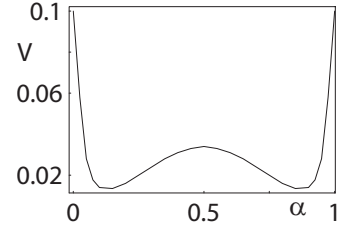


FIG. 10. Here, we present the same thought experiment as in Fig. 9, except that the device is a square with $t_{dev} = t_h$ threaded by a flux ϕ with zero on-site energies. The SQUID-like behavior and the half-fluxon periodicity are lost, as expected in bipartite graphs (see text). In this particular example the lower-left bond was raised to $1.2t_h$ in order to study the effects of a slight deformation of the square, but no relevant departure from the perfect square behavior was found.

a short time. Looking at the current distribution inside the device, $\epsilon_c < 0$ favors a laminar current flow; instead, $\epsilon_c > 0$ produces an anticlockwise current vortex; when a critical value is exceeded, however, the vortex chirality reverses. Further, we have shown that a class of closed circuits at half filling have a degenerate ground state that is paramagnetic, i.e., gains energy in a magnetic field by a Zeeman splitting. The magnetic behavior is completely changed when the circuits are connected to leads and form a nonbipartite lattice. Long leads constitute an essential requirement and although the diamagnetic currents are confined to the ring, the leads modify the magnetic properties substantially. With long enough wires, one obtains a diamagnetic behavior with half-fluxon periodicity and a robust barrier separating the energy minima at 0 and $\phi_0/2$. This pattern mimics a superconducting ring although there are no gap, interactions, or critical temperature. We have traced back the origin of this fake superconducting behavior to a combination of charge-conjugation and flux, which provides a symmetry of the many-electron determinantal state. Finally, we have shown that in principle one can extend this simulation to the point of building a functioning interference device capable of measuring local fields and analogous to a SQUID but working even above room temperature. It cannot be excluded that even-sided circuits can be useful for the same purpose, and, indeed Fig. 10 suggests that one could do so, exploit the trivial periodicity. The signal in Fig. 9, however, is much more monochromatic, and this suggests that the odd-sided version should make it much easier to read off the magnetic field intensity from the amplitude of the voltage oscillation.

¹A. A. Aligia, Phys. Rev. B **66**, 165303 (2002).

²S. Viefers, P. Koskinen, P. Singha Deo, and M. Manninen, Physica E (Amsterdam) **21**, 1 (2004).

³S. Maiti, Solid State Phenom. **155**, 87 (2009).

⁴C. Caroli, R. Combescot, P. Nozieres, and D. Saint James, J. Phys. C **4**, 916 (1971).

⁵M. Cini, Phys. Rev. B **22**, 5887 (1980).

⁶E. Perfetto, G. Stefanucci, and M. Cini, Phys. Rev. B **78**, 155301 (2008).

⁷G. Stefanucci, Phys. Rev. B **75**, 195115 (2007).

⁸G. Stefanucci, E. Perfetto, S. Bellucci, and M. Cini, Phys. Rev. B **79**, 073406 (2009).

⁹M. Ernzerhof, H. Bahmann, F. Goyer, M. Zhuang, and P. Rocheleau, *J. Chem. Theory Comput.* **2**, 1291 (2006).

¹⁰See, for instance, Michele Cini, *Topics and Methods in Condensed Matter Theory* (Springer-Verlag, Berlin, 2007).

¹¹G. S. Canright and S. M. Girvin, *Int. J. Mod. Phys. B* **3**, 1943 (1989).

¹²As noted above, the one-body spectrum is not generally top-down symmetric; at $\alpha=0$, out of the $2\Lambda+3$ eigenvalues, $\Lambda+2$

are negative and $\Lambda+1$ positive; at $\alpha=0.5$, because of the turn-over of the spectrum, $\Lambda+2$ are positive and $L+1$ negative. At $\alpha=0.25$, by a gauge transformation on H one can change the signs of all real bonds, then by complex conjugation one obtains $-H$; since H and H^* must have the same (real) eigenvalues, it follows that one eigenvalue vanishes and the spectrum is top-bottom symmetric like in bipartite lattices.